LAWRENCE
LIVERMORE
NATIONAL
LABORATORY

UCRL-JRNL-203881

Growth of nanocrystalline MoO_3 on Au(111) studied by in-situ STM

M. M. Biener, J. Biener, R. Schalek, and C. M. Friend

April 30, 2004

Submitted to Journal of Chemical Physics B

Disclaimer

This document was prepared as an account of work sponsored by an agency of the United States Government. Neither the United States Government nor the University of California nor any of their employees, makes any warranty, express or implied, or assumes any legal liability or responsibility for the accuracy, completeness, or usefulness of any information, apparatus, product, or process disclosed, or represents that its use would not infringe privately owned rights. Reference herein to any specific commercial product, process, or service by trade name, trademark, manufacturer, or otherwise, does not necessarily constitute or imply its endorsement, recommendation, or favoring by the United States Government or the University of California. The views and opinions of authors expressed herein do not necessarily state or reflect those of the United States Government or the University of California, and shall not be used for advertising or product endorsement purposes.

April 30, 2004
To be submitted to: Journal of Chemical Physics

Growth of nanocrystalline MoO_3 on Au(111) studied by in-situ STM

Monika M. Biener[1,2], Juergen Biener[3,4], Richard Schalek[3], and Cynthia M. Friend[1,2, †]
[1]Department of Chemistry and
[2]Division of Engineering and Applied Sciences and
[3]Center for Imaging and Mesoscale Structures
Harvard University
12 Oxford Street, Cambridge, Massachusetts 02138 USA

[†]Author to whom correspondence should be sent

Abstract

The growth of nanocrystalline MoO_3 islands on Au(111) using physical vapor deposition of Mo has been studied by scanning tunnelling microscopy (STM) and low energy electron diffraction (LEED). The growth conditions affect the shape and distribution of the MoO_3 nanostructures, providing a means of preparing materials with different percentages of edge sites that may have different chemical and physical properties than atoms in the interior of the nanostructures. MoO_3 islands were prepared by physical vapor deposition of Mo and subsequent oxidation by NO_2 exposure at temperatures between 450 K and 600 K. They exhibit a crystalline structure with a c(4x2) periodicity relative to unreconstructed Au(111). While the atomic-scale structure is identical to that of MoO_3 islands prepared by chemical vapor deposition, we demonstrate that the distribution of MoO_3 islands on the Au(111) surface reflects the distribution of Mo clusters prior to oxidation although the growth of MoO_3 involves long-range mass transport via volatile MoO_3 precursor species. The island morphology is kinetically controlled at 450 K, whereas an equilibrium shape is approached at higher preparation temperatures or after prolonged annealing at the elevated temperature. Mo deposition at or above 525 K leads to the formation of a Mo-Au surface alloy as indicated by the observation of embedded MoO_3 islands after oxidation by NO_2. Au vacancy islands, formed when Mo and Au dealloy to produce vacancies, are observed for these growth conditions

Introduction

Nanoparticles and systems in the nanometer size regime have been studied intensively in recent years. These systems may have electronic, optical and catalytic properties which differ considerably from those of the corresponding bulk material and depend strongly on the size and morphology of the structures. For example gold nanoparticles dispersed on metal oxides are chemically active,[1, 2] whereas gold is inert as bulk material. Another example is molybdenum: Mo clusters on gold exhibit a very low activity towards O_2 and CO,[2, 3] whereas bulk Mo dissociates CO and O_2 below 300 K.[4, 5] Hence, an understanding of the growth mechanism and the capability to control the morphology of nanoscopic systems is an important step towards the development of materials with unusual chemical and physical properties.

Considerable interest has been focused on metal oxides because of their broad range of physical and chemical properties and their applications in technology, catalysis and environmental protection. In particular, molybdenum trioxide is known to promote the partial oxidation of methane to formaldehyde.[6-9] Stoichiometric MoO_3 has a bandgap of 2.8 eV, however, states are introduced in the gap when point defects due to loss of oxygen are created.[10] Catalytic activity is often attributed to the presence of oxygen vacancies associated with edge sites of the material.[11]

Recently, the growth of 2D vanadium and iron oxides on metal surfaces has been reported. On Pd(111), a metastable two-dimensional V_2O_3 phase is formed in the submonolayer coverage regime.[12] The morphology of this oxide phase strongly depends on the preparation conditions and is different from the bulk V_2O_3 structure. Similarly, metastable FeO(111) films can be grown on Ru(0001).[13] These studies clearly demonstrate that non-equilibrium metal oxide phases can be stabilized on metal surfaces.

The formation of nanocrystalline MoO_3 islands using chemical vapor deposition (CVD) of Mo has recently been investigated by our group.[14] Briefly, preferential nucleation of Mo clusters at Au step edges was achieved by CVD of Mo using $Mo(CO)_6$ as a precursor. Subsequent exposure of these Mo clusters to NO_2 at 450 K leads to the growth of nanocrystalline MoO_3 islands, which nucleate preferentially at the step edges. Both scanning tunnelling microscopy (STM) and low energy electron diffraction (LEED) data reveal a well defined c(2x4) superlattice.

In this paper we demonstrate that the spatial distribution of the Mo clusters dictates the initial nucleation sites and the morphology of MoO_3 islands. In particular, nucleation of crystalline MoO_3 islands *on* Au(111) terraces was observed after oxidation of ordered 2D arrays of Mo nanostructures by NO_2 exposure. Such ordered arrays of Mo nanostructures can be prepared by physical vapor deposition (PVD) of Mo, and are a consequence of the preferred nucleation of Mo at elbow sites of the reconstruction of the Au(111) surface. The spatial distribution of the Mo clusters controls the initial nucleation sites of MoO_3 islands despite the fact that long-range mass transport is necessary to explain the observed growth kinetics. Furthermore we show that the exact morphology of the MoO_3 islands strongly depends not only on the deposition method but also on other preparation conditions such as deposition, oxidation and annealing temperature.

Experimental

All experiments were performed in a commercial ultrahigh vacuum (UHV) system with a base pressure of $5x10^{-11}$ mbar. The system has separate compartments for sample preparation, e.g. Mo evaporation, and sample characterization. The characterization compartment is equipped with commercial instrumentation for scanning probe microscopy (SPM) (Omicron), Auger electron spectroscopy (AES) and low energy electron diffraction (LEED).

The Au(111) sample was cleaned by repeated cycles of sputtering with 1000 eV energy Ar^+ for 60 minutes with an ion current of 4 μA at room temperature. Subsequently the sample was annealed for 10 min at 900 K followed by one hour at 700 K. This procedure was repeated until no contaminants were detected by means of AES. The sample was radiatively heated, and the temperature was monitored using a Cr-Al thermocouple attached to the manipulator. Initially the temperature was calibrated by a Cr-Al thermocouple spot-welded to a sample holder plate. Annealing times given in the text do not include the ramp-up time which was typically ~ 10 minutes.

Molybdenum (Goodfellow, 99.9%) was evaporated from rod material (1.5 mm diameter) using an electron beam evaporator (Omicron) (900 V / ~ 65 mA). The deposition rate was monitored continuously by a flux monitor measuring the ion flux, which is approximately proportional to the flux of evaporated atoms. Using the flux monitor to determine the exposure, a specific coverage could be achieved with a reproducibility of +/- 10 %. Initially the deposition rate was calibrated using a quartz thickness monitor. All preparations in this publication were performed using a flux of ~0.25 to 0.75 ML Mo min^{-1}. Evaporated molybdenum was oxidized by exposure to nitrogen dioxide (Matheson, 99.5%) at a typical pressure of 1-2 x 10^{-7} mbar. The purity of NO_2 was periodically checked with a residual gas analyzer.

STM images were collected either at room temperature or at elevated temperatures (if indicated), and Z-channel (topography) and I-channel (constant height) images were obtained simultaneously. Etched $Pt_{0.8}$ $Ir_{0.2}$ tips from Molecular Imaging were used for imaging.

Results and Discussion

Nanocrystalline, single-layer MoO_3 islands are formed on terraces of the Au(111) surface after oxidation of Mo cluster arrays by exposure to NO_2 at 600 K (Figure 1). The arrays of Mo nanoclusters were prepared by PVD at temperatures between 450 K and 600 K. As recently reported[15] and reproduced in our laboratory[16] Mo clusters prepared by PVD nucleate preferentially at the elbow sites of the herringbone reconstruction. Subsequent oxidation of these Mo clusters leads to nucleation of MoO_3 islands on Au(111) terraces. Specifically, the MoO_3 islands shown in figure 1a were prepared by deposition of 0.3 ML Mo at 600 K and subsequent exposure to 20 L NO_2 at 600 K. The nucleation of MoO_3 *on* terrace sites is in contrast to the step-edge decoration observed in our previous study of MoO_3 using CVD of the Mo.[14]

The MoO_3 islands have a well-defined crystalline structure with a c(4x2) unit cell, based on our STM and LEED data (figure 2). The LEED pattern displayed in figure 2a is identical to the LEED pattern previously observed from MoO_3 islands on Au(111) prepared by CVD.[14] High resolution STM data reveal a rectangular unit cell with dimensions of 0.50 x 0.57 nm^2 ± 10% (figure 2b), consistent with the observation of the c(2x4) LEED pattern. Thus the atomic structure of MoO_3 islands prepared by PVD is identical to the structure of MoO_3 islands using CVD to deposit the Mo.[14] MoO_3 on Au(111) forms a single layer structure which differs from the bilayer structure of bulk MoO_3.[17] The single layer MoO_3 islands exhibit an apparent height of ~ 0.5 nm and the atomic structure can be explained in terms of an ordered, two-dimensional array of interacting MoO_3 entities. X-ray photoelectron experiments revealed that the predominant oxidation state of Mo (> 90%) in single layer molybdenum oxide islands prepared on Au(111) is +6.[18]

STM images of individual islands often reveal defect structures (indicated by arrows in fig 2b); sometimes, in a quasi-regular superlattice. Repeated scanning of an island leads to an increase in the defects present, suggesting that the STM tip may induce additional defects. Ordered arrays of defects are commonly caused by the presence of strain, as for example the herringbone reconstruction of the Au(111) surface. Indeed, density functional theory calculations reveal that the in-plane Mo-O bonds of single layer MoO_3 on Au(111) are longer than the corresponding equilibrium M-O bonds in bulk MoO_3, suggesting a compressive stress. X-ray photoelectron data show that most of the Mo is in the +6 oxidation state, but that ~10% has a +5 oxidation state indicating the existence of defects.

The MoO_3 islands on terrace sites reflect the symmetry of the Au(111) surface, based on our STM and LEED measurements (figures 1, 2). The islands shown in figure 1a have a characteristic, hexagonal shape with a typical aspect (length : width) ratio of ~ 2.5. The long island edges run parallel to the herringbone structure of the Au(111) surface, i.e. parallel to the [11-2] directions of the underlying substrate. In some instances, rotational domains coalesce as they grow to form “sock-like” structures with a 120 degree bend, reflecting the three-fold symmetry of the underlying Au. Quantitative analysis of STM images reveals a relatively narrow distribution of the island width exhibiting a peak at 18.5 nm, corresponding to 3 times the width of the herringbone structure.

The elongated shape of the MoO_3 islands on the terraces is a consequence of kinetic control of the growth. Indeed, the elongated nanostructures grown at 600 K assume a more compact shape after annealing at 600 K for 10 minutes (Figure 1b), clearly indicating the role of growth kinetics in the formation of the anisotropic shapes. The anisotropic growth could be due to anisotropic step edge diffusion,[19] i.e. different diffusion barriers for the growth species along the short and long edges of the MoO_3 islands. Specifically, the observed island shape implies a higher diffusion barrier of MoO_3 precursor species along the short island edges than along the long edges. This leads to a higher density of MoO_3 precursor species at short island edges, and thus to a higher nucleation probability. Furthermore the observation that the island width correlates with the width of the herringbone, as mentioned above, suggests that the

diffusion barriers depend not only on the orientation but also on the position of the island edge with respect to the reconstruction.

The formation of MoO_3 islands leads to a lifting of the reconstruction under the islands, based on STM data. Specifically, the characteristic herringbone structure becomes disrupted and avoids the oxide islands (Figure 1 insert). Occasionally "U-turns" of the herringbone pattern were observed. It is well known that the interaction with adsorbates can lift the herringbone reconstruction.[20, 21] Note that the lifting of the reconstruction of the Au under the oxide nanostructure creates a boundary between reconstructed and unreconstructed regions of the Au that could affect growth kinetics.

The morphology of the MoO_3 islands depends strongly on the Mo deposition temperature. Specifically, the formation of "embedded" MoO_3 islands on Au(111) was observed if the Mo was deposited at or above 525 K, as exemplified in the STM image obtained from a preparation at 600 K (Figure 3). The embedded MoO_3 islands can be identified by their reduced apparent height as illustrated by the line scan shown in the insert. The crystalline structure of the embedded MoO_3 islands is identical to those growing on top of the Au terrace; however, the shape of the two types of MoO_3 islands is different: island A is embedded and has a round shape, whereas island B grows free on the terrace and has the shape of an elongated hexagon.

We attribute the formation of these embedded MoO_3 islands to vacancy formation via NO_2 induced de-alloying of a Mo-Au surface alloy. In other work, we found evidence for the formation of a substitutional Mo-Au surface alloy during Mo deposition at or above 525 K.[16] Subsequent oxidation of Mo triggers de-alloying, and the vacancies generated in this step aggregate into "vacancy islands" in the Au surface. These vacancy islands then serve as nucleation sites for the growth of MoO_3 islands, or annihilate at step edges. The fact that Au vacancy islands were not observed within a distance of ~150 nm from the step edges at 600 K is an indication of the diffusion length of the vacancies. We attribute the difference in shape to the imposition of boundary conditions on the growth of embedded MoO_3: vacancy islands dictate the shape of MoO_3 islands growing inside a vacancy island. Thus, the shape of the embedded MoO_3 islands is significantly different from the shape of MoO_3 islands formed without boundary conditions *on* the terraces.

The observation of partially filled vacancies in case of lower deposition and oxidation temperature suggests a diffusion-limited growth regime. Partially filled vacancy islands (VI in Fig 4) were observed after deposition of 0.3 ML of Mo at 525 K and subsequent oxidation by 20 L NO_2 exposure at 525 K. As observed when MoO_3 is prepared at 600 K, the islands nucleate at the step edges of the vacancy islands; however, the ripening process is slower at 525 K, and the mass transport of MoO_3 precursor species by surface diffusion is insufficient to completely fill the vacancy island. Thus the individual MoO_3 islands within a vacancy island do not coalesce within the annealing time. Occasionally, the herringbone pattern within a vacancy island could be resolved (fig 4b insert), confirming that the vacancy islands are in Au itself. Furthermore the density of small MoO_3 islands increases compared to the 600 K preparation described above. The height of an embedded MoO_3 island and a MoO_3 islands *on* the terrace is identical (fig 4a) with respect to the underlying Au.

Kinetic control of the island growth is even more pronounced if the Mo clusters are oxidized at 450 K. While the regular, hexagonal shapes obtained after oxidation at 525 K and 600 K indicate that diffusion is sufficiently fast to approach an ordered state, oxidation at lower temperature leads to irregular shapes that indicate that the growth is kinetically limited. For example, islands with less well-defined edges are obtained after oxidation of Mo (0.3 ML) deposited at 450 K and subsequently oxidized by exposure to 20 L NO_2 at 450 K (Figure 5). Most noteworthy is the large fraction of small islands and the ramified shape of the larger islands which exhibit a typical aspect ratio of approximately five with the long edge aligned parallel to the [11-2] directions of the Au(111) surface. In contrast to deposition and oxidation at 525 K or higher, vacancy islands are not observed. Instead, the formation of small Au islands is observed, which can, like step edges, serve as nucleation sites for MoO_3 islands. These Au islands can be identified by the herringbone pattern (fig 5a inserts).

Our previous investigations [14, 16] suggest that some Au atoms are incorporated into the Mo clusters. Subsequent oxidation of the Mo clusters causes de-alloying, and the Au atoms released during this step then lead to the formation of small Au islands (fig 5a insert). Alternatively, the Au islands might originate from the additional Au atoms of the herringbone reconstruction, which is lifted underneath the MoO_3 islands. A quantitative analysis is, however, not possible as the fraction of Au atoms which are released by the processes described above and form Au islands is unknown.

Ostwald ripening of the MoO_3 nanostructures is observed during annealing. Specifically, the irregular and elongated MoO_3 islands created by deposition and oxidation at 450 K assume a less anisotropic shape upon heating to 650 K for 10 minutes (fig. 5 b). No loss of MoO_3 was observed during annealing to 650 K based on AES data (not shown). These changes are consistent with those observed if MoO_3 prepared at 600 K and subsequently imaged at room temperature (fig. 1a) was further annealed at 600 K for 10 minutes (fig. 1b).

The more compact shape should be more thermodynamically stable than an elongated irregular shape because the ratio of the perimeter length to area is smaller; thus, the number of unstable edge sites is reduced. Besides the change in shape, the islands also change in size: larger islands grow at the expense of smaller islands. The observed change of the island shape towards a more compact shape confirms our assertion that the elongated hexagonal shape observed prior to annealing is the result of anisotropic diffusion and, therefore, indicates kinetic control. The conversion towards the more stable island morphology is a slow process, even at 600 K, and requires further annealing after oxidation. According to STM and LEED the unit cell structure of the MoO_3 islands is unaffected by the annealing to 650K. However, higher temperatures (700 K and above) lead to thermal reduction and the formation of shear planes as described elsewhere.[22]

The growth mechanism of the MoO_3 islands was further investigated by in-situ STM. Mo clusters (0.3 ML) were deposited on Au(111) at 500 K and subsequently oxidized by incremental NO_2 exposure at 500 K. STM images were collected *at* 500 K between each oxidation step and are shown in fig. 6. During NO_2 exposure the STM tip was retracted, as otherwise a tip shadowing effect in terms of a reduced oxidation rate was observed. In the initial reaction regime the apparent height of the Mo clusters increases from 0.5 nm to 1 nm with increasing NO_2 exposure. Simultaneously, the long-

range order of Mo cluster arrays diminishes. However, the unimodal size distribution of the Mo clusters remains. Starting at an exposure of ~14L NO_2, 2D MoO_3 islands are observed to nucleate, initially at step edges and later on the terraces. A local depletion of Mo clusters around growing MoO_3 islands was not observed. With increasing NO_2 fluence the MoO_3 islands grow in size, and finally the Mo cluster density starts to decrease.

The observed growth kinetic of the MoO_3 islands indicates a non-local, long-range mass transport of MoO_3 precursor species from oxidized Mo clusters to growing MoO_3 islands. The nearly constant Mo cluster density in the initial MoO_3 growth regime reveals that existing Mo clusters contribute evenly by 2D evaporation of volatile $(MoO_3)_x$ species to the observed mass transport; premature dissolution of individual Mo clusters in the vicinity of growing MoO_3 islands, i.e. the formation of a depletion zone, was not observed. A quantitative analysis of the experiment demonstrates that the initially uniform Mo coverage of ~0.3 ML (e.g. in fig. 6a) transforms into a local coverage of 0.5 ML MoO_3 on the narrow terrace running through the center of the image in figure 6d. This observation reveals that long-range mass transport takes place even across steps. This long-range mass transport was also observed in our previous study of the MoO_3 formation using CVD. It is remarkable that the spatial distribution of the Mo clusters influences the spatial distribution of MoO_3 islands although long-range mass transport is a prerequisite to explain the observed growth kinetics.

This work provides a guide for synthesizing MoO_3 nanostructures with specific shapes and distributions on the Au surface. By controlling the shape and distribution of the islands on the surface, we are able to create different bonding environments that may affect the chemical and physical properties of the nanostructures. In particular, atoms at the periphery of the nanostructures have different bonding environments and coordination and may, therefore, have different chemical properties than in interior. Furthermore, we are able to create and image specific defects in these oxides that may create reactive centers or change the electronic and optical properties of these materials. We are currently investigating the chemical and physical properties of these materials to address these points.

Conclusion

Nanocrystalline MoO_3 islands on Au(111) terraces can be synthesized by PVD of Mo followed by oxidation using NO_2. Both shape and spatial distribution of the MoO_3 islands are in sharp contrast to the results of our previous investigations using a CVD approach to deposit molybdenum. CVD leads to preferential nucleation of MoO_3 at step-edges, and both island shape and orientation are dictated by boundary conditions induced by the presence of substrate step-edges. The main difference between the PVD approach described in this paper and the CVD approach reported earlier is the spatial distribution of the Mo clusters on the Au(111) surface prior to oxidation: terrace (PVD) versus step-edge decoration (CVD), respectively. Hence, the spatial distribution of the Mo clusters controls the initial nucleation sites of MoO_3 islands despite the fact that long-range mass transport is necessary to explain the observed growth kinetics.

Furthermore the morphology of the MoO_3 islands strongly depends on deposition and oxidation temperatures. For deposition temperatures at 525 K or above we observe NO_2 induced dealloying of a Mo-Au surface alloy formed during Mo deposition. This, in turn, leads to the observation of "embedded" MoO_3 islands, which nucleate at steps of Au vacancy islands. The oxidation temperature affects the growth kinetics of MoO_3 islands: diffusion of MoO_3 precursor species is kinetically controlled at 450 K, which leads to an irregular shape of MoO_3 islands with a high aspect ratio. With further annealing the islands change in size and shape via Ostwald ripening.

The ability to synthesize nanostructures with different distributions and shapes is important for understanding how edge sites present in small structures and modification of materials due to boundary conditions imposed by the substrate affect chemical and physical properties. These issues are central to understanding complex, integrated nanostructures.

Acknowledgements:

We gratefully acknowledge the support of this work by the US Department of Energy, Basic Energy Science, under grant number DE-FG02-84ER13289 and by the Harvard University NSEC, funded by the National Science Foundation, grant no. PHY-01-17795. J.B. acknowledges current support under the auspices of the U. S. Department of Energy by the University of California, Lawrence Livermore National Laboratory, under Contract No. W-7405-Eng-48.

Figure Captions:

Figure 1: STM image (I-channel) showing nanocrystalline MoO_3 islands on Au(111) after Mo deposition and subsequent oxidation by NO_2 exposure at 600 K (a).The islands nucleate predominantly on terraces and reveal a hexagonal shape with a high aspect ratio. The island edges are aligned with the [11-2] direction of the substrate. Further annealing at 600 K for 10 minutes leads to a more compact island shape (b). The images were obtained at 300 K and correspond to an area of 500 nm x 500 nm (insert in (a): 70 nm x 70 nm).

Figure 2: Identification of the c(4x2) unit cell of the MoO_3 islands on Au(111) prepared by PVD of Mo and subsequent oxidation with NO_2 at 600 K: (a) LEED pattern obtained at 300 K revealing a c(4x2) structure, and (b) high resolution STM image (7 nm x 7 nm) showing a rectangular unit cell with a = 0.50 nm and b = 0.57 nm ±10%, obtained at 300 K. Defects are indicated by arrows.

Figure 3: STM image showing two different types of MoO_3 islands prepared at 600K: island A is embedded and has a round shape, island B is on the terrace and has the shape of an elongated hexagon. A line scan along the indicated section is shown in the insert and illustrates the difference in the apparent height. The image corresponds to an area of 500 nm x 500 nm.

Figure 4: STM images showing MoO_3 islands on Au(111) after Mo deposition and subsequent oxidation by NO_2 exposure at 525 K: (a) Vacancy islands (VI) on Au(111) partially filled with MoO_3. A line scan along the indicated section is shown in the insert and illustrates that the height of MoO_3 islands in vacancy islands and MoO_3 islands *on* terraces are identical with respect to the underlying Au. (b) STM image (I-channel) showing the alignment of the MoO_3 islands and the Au(111) reconstruction pattern in a vacancy island (insert). The images correspond to an area of 250 nm x 250 nm (insert 83 nm x 83 nm).

Figure 5: STM images demonstrating Oswald ripening of MoO_3 islands on Au(111): (a) After deposition at 450 K MoO_3 islands are irregularly shaped; occasionally small Au islands are observed which can be identified by their reconstruction pattern (see inserts in I and Z channel, respectively). (b) A more compact MoO_3 island morphology is observed after annealing to 650 K for 10 min. The images correspond to an area of 500 nm x 500 nm, the inserts to 33 nm x 33 nm.

Figure 6: STM images illustrating the growth mechanism of MoO_3 islands at 500 K. Mo was deposited at 500 K and STM images were collected in-situ at 500 K between incremental oxidation steps at 500 K. The NO_2 fluence is: (a) 10 L, (b) 16 L, (c) 18 L,

(d) 20 L, and (e) 34 L. With increasing NO_2 flux the MoO_3 islands initially nucleate at the step edges and later on the terraces. The cluster density is unchanged in the vicinity of the growing MoO_3 islands indicating long-range mass transport. All images correspond to an area of 200 nm x 200 nm.

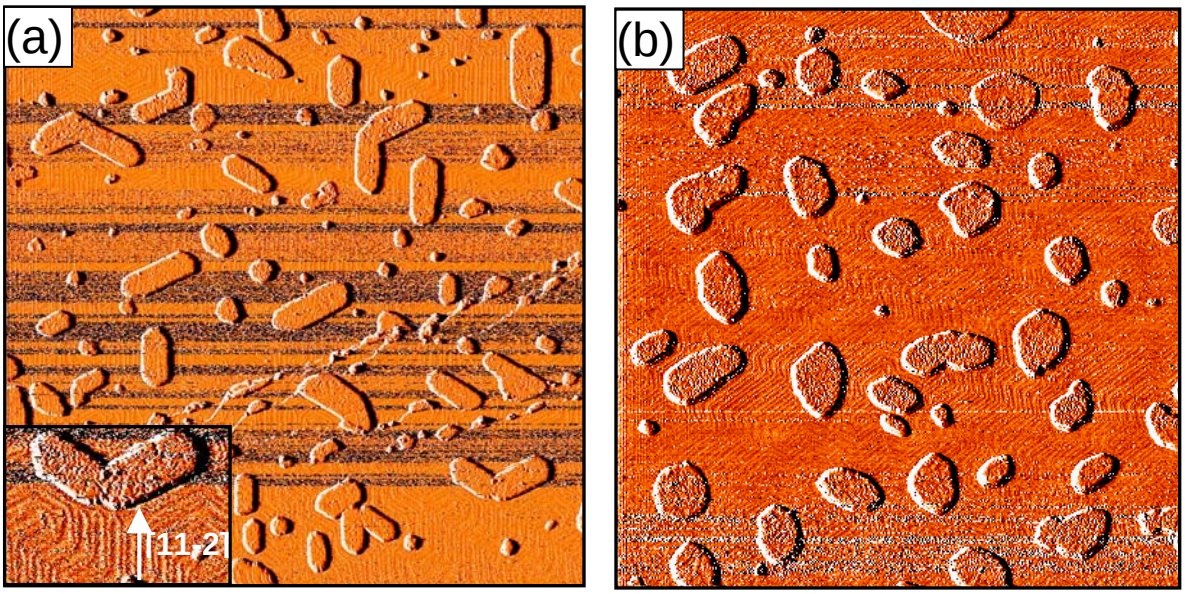

Figure 1

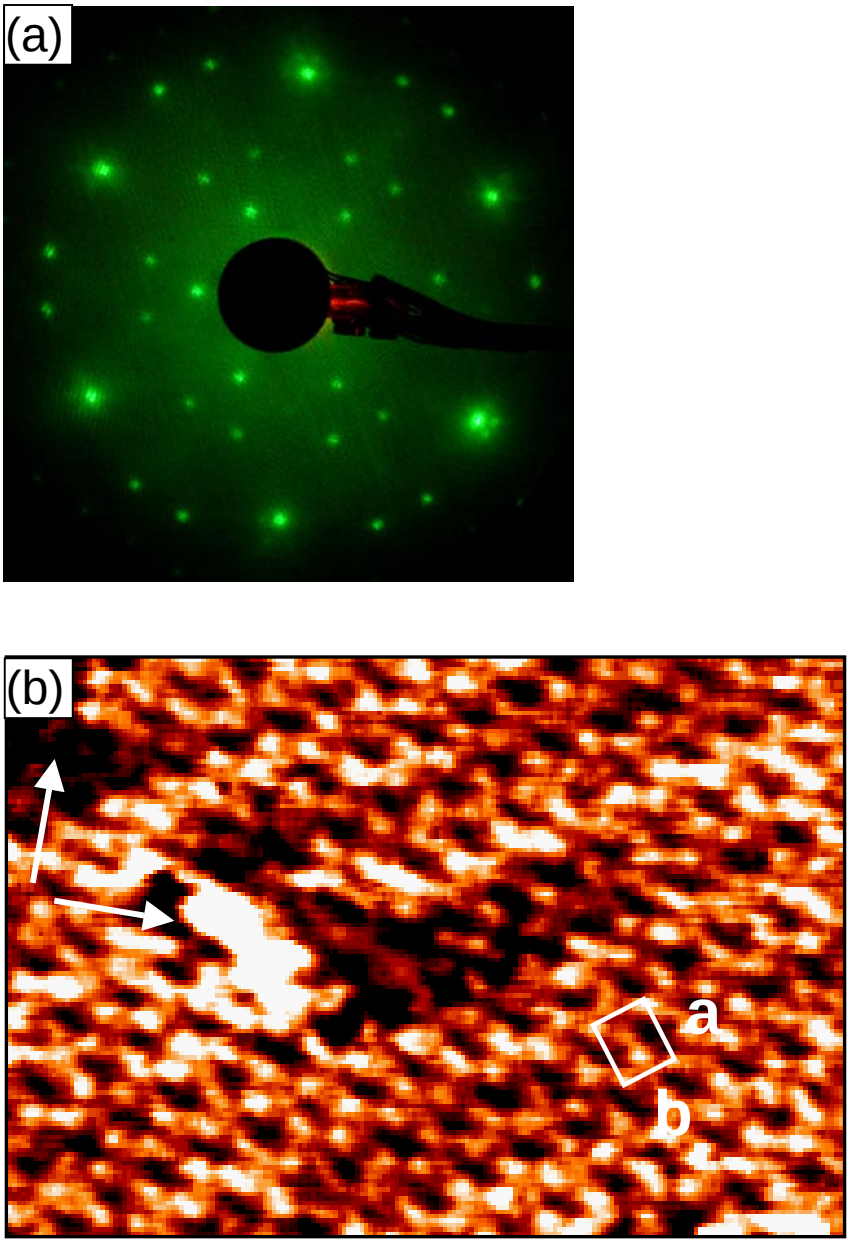

Figure 2

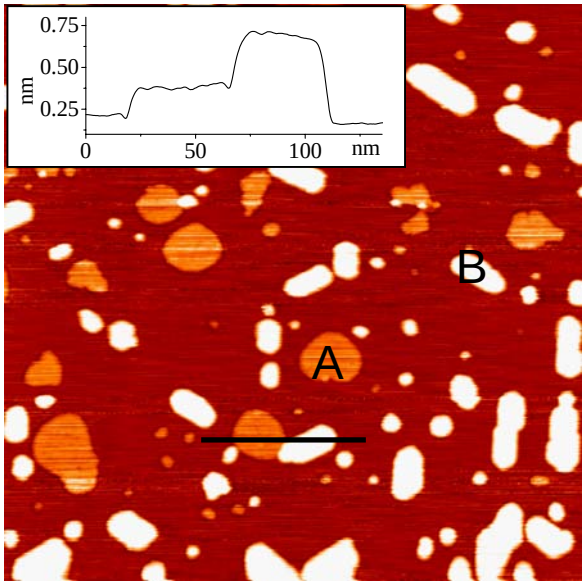

Figure 3

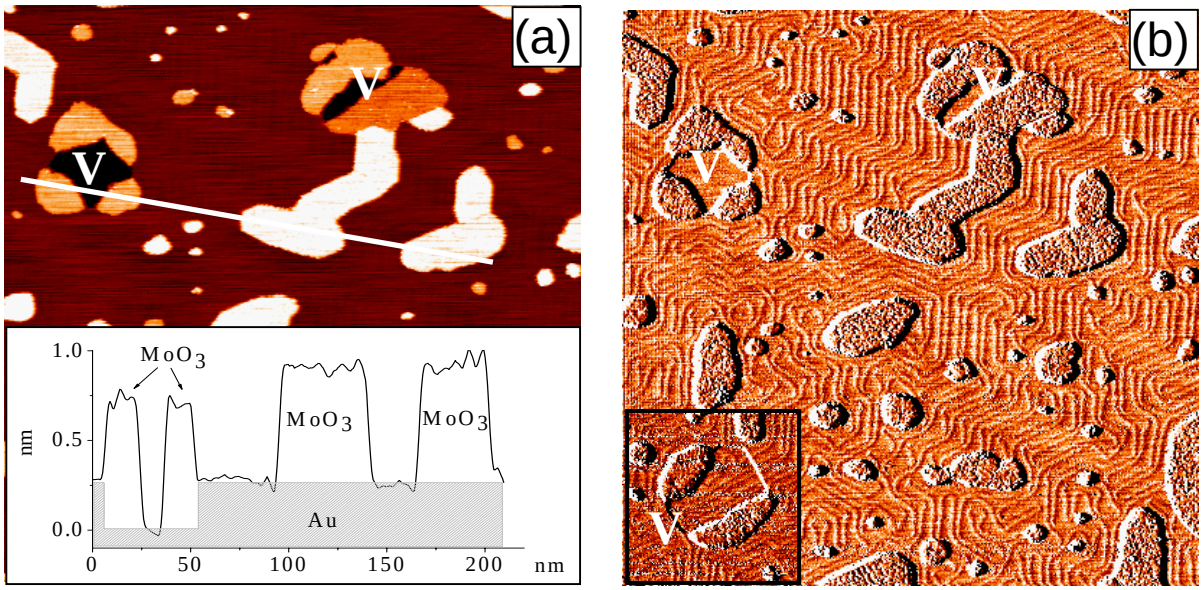

Figure 4

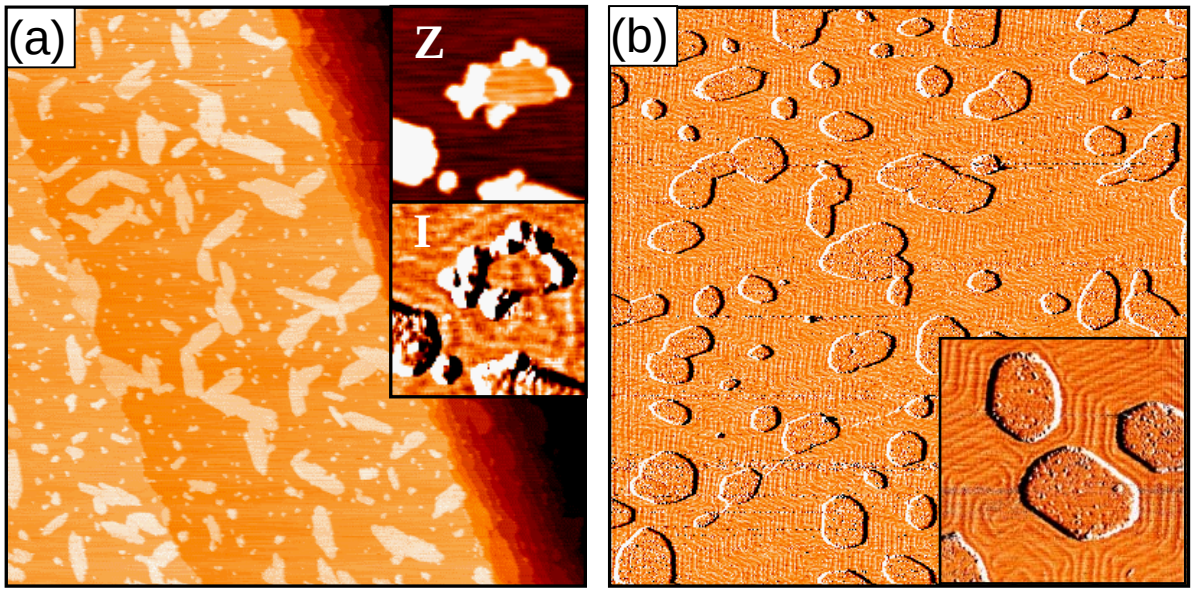

Figure 5

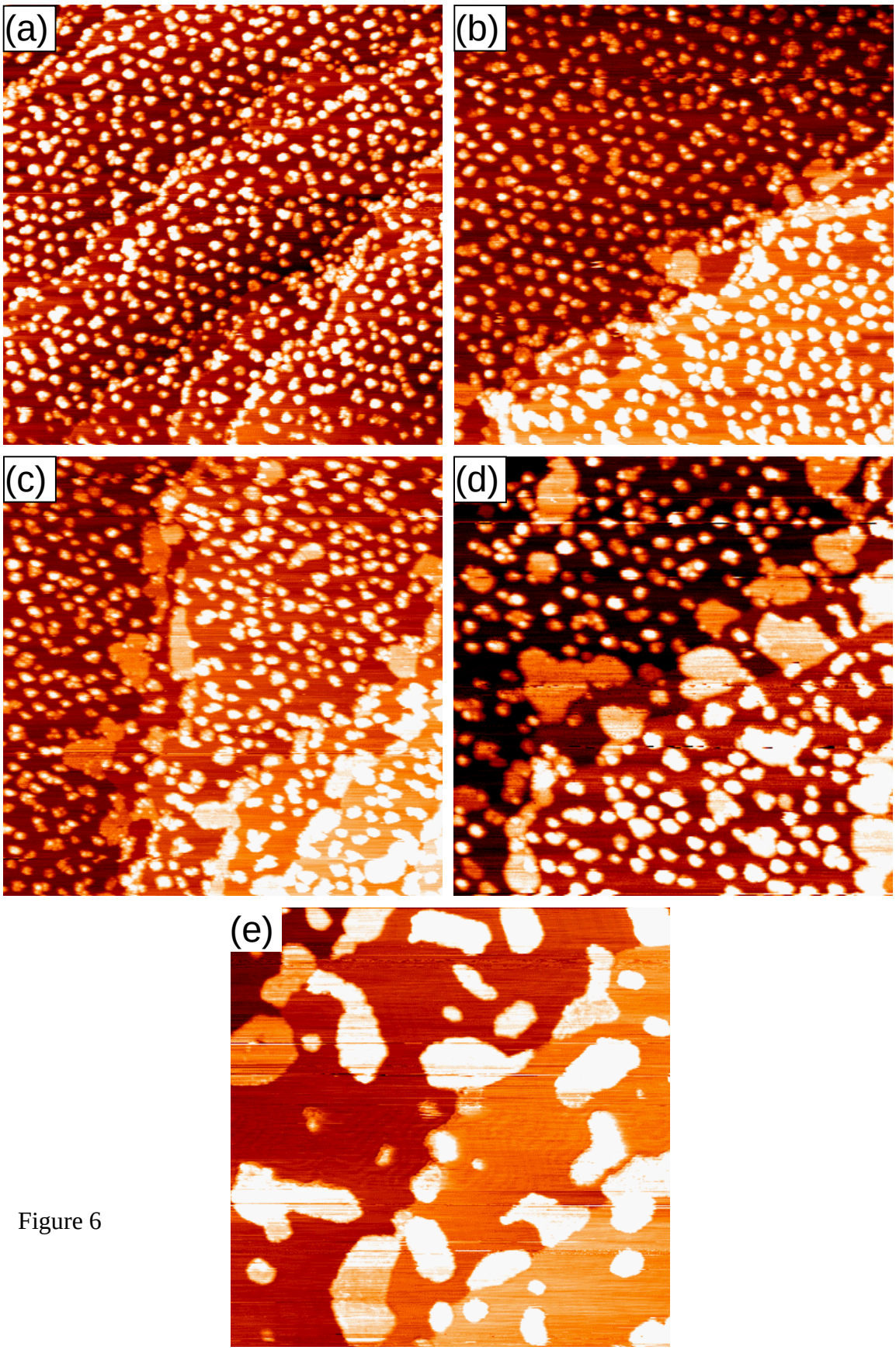

Figure 6

References

[1] M. Valden, X. Lai, and D. W. Goodman, Science **281**, 1647 (1998).
[2] Z. P. Chang, Z. Song, G. Liu, et al., Surface Science **512**, L353 (2002).
[3] J. A. Rodriguez, J. Dvorak, T. Jirsak, et al., Surf. Sci. **490**, 315 (2001).
[4] A. J. Jaworowski, M. Smedh, M. Borg, et al., Surface Science **492**, 185 (2001).
[5] G. H. Smudde and P. C. Stair, Surf. Sci. **317**, 65 (1994).
[6] P. J. Spencer, United States Patent **4,607,127** (1986).
[7] N. D. Spencer and C. J. Pereira, AIChE Journal **33**, 1808 (1987).
[8] N. D. Spencer, Journal of Catalysis **109**, 187 (1988).
[9] M. A. Banares, N. D. Spencer, M. D. Jones, et al., J.Catal. **146**, 204 (1994).
[10] M. Chen, C. M. Friend, and E. Kaxiras, JACS (2001).
[11] J. Haber and E. Lalik, Catal. Today **33**, 119 (1997).
[12] S. Surnev, L. Vitali, M. G. Ramsey, et al., Phys. Rev. B **61**, 13945 (1999).
[13] G. Ketteler and W. Ranke, J. Phys. Chem. B **107**, 4320 (2003).
[14] M. M. Biener and C. M. Friend, Surface Science Letters (in press).
[15] S. Helveg, J. V. Lauritsen, E. Laegsgaard, et al., Phys. Rev. Lett. **84**, 951 (2000).
[16] M. M. Biener, J. Biener, R. Schalek, et al., Phys. Rev. B (submitted).
[17] E. Itoh, K. Hayakawa, and S. Oishi, J. Phys.: Condens. Matter **13**, 6853 (2001).
[18] X. Deng, D.-H. Kang, J. Biener, et al., (in preparation).
[19] T. Michely, M. Hohage, M. Bott, et al., Phys. Rev. Let. **70**, 3943 (1993).
[20] D. Krznaric, T. Goricnik, and B. Cosovic, Croatica Chemica Acta **73**, 247 (2000).
[21] S. Strbac, O. M. Magnussen, and R. J. Behm, J. Serb. Chem. Soc. **66**, 119 (2001).
[22] M. M. Biener, J. Biener, and C. M. Friend, (to be published).